Upper critical field, superconducting energy gaps and the Seebeck coefficient in $La_{0.8}Th_{0.2}FeAsO$

2009 J. Phys.: Condens. Matter 21 175705

(http://iopscience.iop.org/0953-8984/21/17/175705)

J. Phys.: Condens. Matter **21** (2009) 175705 (6pp) doi:10.1088/0953-8984/21/17/175705

Upper critical field, superconducting energy gaps and the Seebeck coefficient in $La_{0.8}Th_{0.2}FeAsO$

J Prakash[1], **S J Singh**[2], **S Patnaik**[2,3] **and A K Ganguli**[1,3]

[1] Department of Chemistry, Indian Institute of Technology, New Delhi 110016, India
[2] School of Physical Sciences, Jawaharlal Nehru University, New Delhi 110067, India

Received 8 January 2009, in final form 21 February 2009
Published 1 April 2009
Online at stacks.iop.org/JPhysCM/21/175705

Abstract

We report the synthesis and characterization of a new electron-doped La-oxypnictide superconductor by partial substitution of lanthanum by thorium. The superconducting transition temperature at about 30.3 K was observed in $La_{0.8}Th_{0.2}FeAsO$, which is the highest in La-based oxypnictide superconductors synthesized at ambient pressure. We find that the decrease in lattice parameters with Th doping in LaOFeAs is more drastic as compared to that obtained by high pressure (6 GPa) synthesis of oxygen-deficient LaOFeAs. The resistivity and magnetic susceptibility measurements yield an upper critical field $H_{c2}(0)$ of 47 T. Partial substitution of Th in place of La induces electron doping, as shown by a negative Seebeck coefficient. The temperature-dependent magnetic penetration depth data provides strong evidence for a nodeless low energy gap of 1.4 meV.

(Some figures in this article are in colour only in the electronic version)

1. Introduction

The recent discovery of superconductivity in layered rare-earth transition metal (Ln) oxypnictides of the type LnFeAsO has given rise to immense interest in the field of high temperature superconducting materials. Kamihara *et al* first showed that the iron-based compound LaFeAsO exhibits superconductivity with a transition temperature of 26 K by partial substitution of oxygen by fluorine [1]. Detailed band structure calculations in this novel class of superconductors indicate that the ground state of these materials corresponds essentially to a low carrier density metal with disconnected Fermi surfaces and in close proximity to an itinerant magnetic state, in particular a spin density wave (SDW) correlation at around 150 K. It is proposed that superconductivity is induced by the suppression of the SDW state through electron doping [2–5]. This has led to T_c being increased up to 55 K with the replacement of La by the smaller rare earths Ce, Sm, Nd, Pr and Gd [6–10]. These are the first noncopper materials that exhibit superconductivity above 50 K.

The oxypnictides LnFeAsO crystallize in the layered tetragonal ZrCuSiAs structure (space group: $P4/nmm$) with alternating layers of La–O and Fe–As. The ionic La–O layer acts as a charge reservoir and the Fe–As layer acts as a charge carrier [11]. We have earlier reported the potassium fluoride-doped La-based oxypnictide with nominal composition $La_{0.8}K_{0.2}FeAsO_{0.8}F_{0.2}$ which shows a superconducting transition around 26.5 K [12]. The above superconductors are mainly induced by electron doping by substitution of F^- ions in place of O^{2-}. There have also been reports [13] of Co doping at Fe sites to induce superconductivity. Recently Wang *et al* have established another route for electron doping, e.g. substitution of Th^{4+} in place at the Ln (rare-earth) site in LnFeAsO (Ln = Gd, Tb). This has led to superconductivity at 56, 50 and 38 K in (Gd/Th)FeAsO, (Tb/Th)FeAsO and (Nd/Th)FeAsO, respectively [14–16]. In this paper, we have investigated the effect of thorium doping at the lanthanum site in (LaFeAsO) on its electrical and magnetic properties. The spin density wave state is completely suppressed upon Th doping and a superconducting transition is observed at 30.3 ($\pm$0.05) K in $La_{0.8}Th_{0.2}FeAsO$, which is the highest T_c reported in La-based oxypnictides synthesized at ambient temperature. We also report our investigation on La-and O-deficient compounds of the type $La_{1-\delta}FeAsO$ and $LaFeAsO_{1-\delta}$ ($\delta \leqslant 0.2$). The thermodynamic parameters, such as the upper critical field

[3] Authors to whom any correspondence should be addressed.

and coherence length, have been estimated. The temperature dependence of rf penetration depth exhibits strong evidence in support of an exponential isotropic pairing mechanism.

2. Experiment

Polycrystalline samples with nominal compositions of $La_{1-x}Th_xFeAsO$ ($x = 0.1$ and 0.2), $La_{1-\delta}FeAsO$ ($\delta = 0.1$ and 0.2) and $LaFeAsO_{1-\delta}$ ($\delta = 0.1$ and 0.2) were synthesized by the conventional solid state reaction method [12, 17] using high purity La, La_2O_3, ThO_2 and FeAs. FeAs was obtained by heating Fe and As chips in evacuated sealed silica tubes at 800 °C for 24 h. The reactants were taken in stoichiometric ratio and sealed in evacuated silica (10^{-4} Torr) tubes and heated at 950 °C for 24 h. The resulting powder was ground and compacted into discs. The discs were wrapped in Ta foil and sealed in evacuated silica ampoules. The compacted discs were sintered at 1180 °C for 48 h and then cooled to room temperature. All the materials were handled in a nitrogen-filled glove box. The samples were characterized by powder x-ray diffraction (XRD) using Cu Kα radiation. The lattice parameters were obtained from a least-squares fit to the observed d values.

The resistive and magnetic measurements were carried out using a cryogenic 8 T cryogen-free magnet in conjunction with a variable temperature insert (VTI). The electrical properties were studied by the standard four-probe technique. Contacts were made using 44 gauge copper wires with air drying conducting silver paste. For magnetic measurements, the magnetic field (0–5 T) was applied perpendicular to the probe current direction and the data were recorded during the warming cycle with a heating rate of 1 K min^{-1}. The inductive part (real part) of the magnetic susceptibility was measured via a tunnel-diode-based rf (2.3 MHz) penetration depth technique [18] attached to this cryogen-free magnet system. A change in magnetic state of the sample results in a change in the inductance of the coil and is reflected as a shift in the oscillator frequency which is measured by an Agilent 53131A counter. Energy-dispersive analysis by x-rays (EDX) was carried out on sintered pellets of the compounds on a Zeiss electron microscope in conjunction with a Bruker EDX system. The thermoelectric power (TEP) data were obtained in the bridge geometry across a 2 mm × 3 mm platelet.

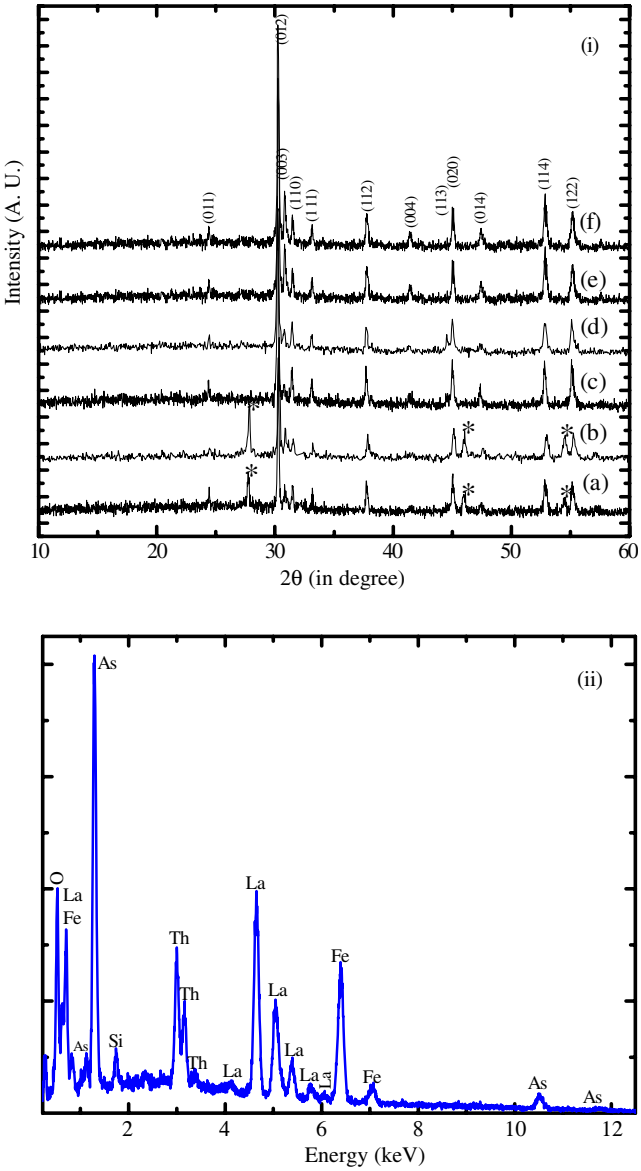

Figure 1. (i) Powder x-ray diffraction patterns (XRD) of (a) $La_{0.9}Th_{0.1}FeAsO$, (b) $La_{0.8}Th_{0.2}FeAsO$, (c) $La_{0.9}FeAsO$, (d) $La_{0.8}FeAsO$, (e) $LaFeAsO_{0.9}$ and (f) $LaFeAsO_{0.8}$ sintered at 1180 °C. The impurity phases are ThO_2 (∗). (ii) EDX spectrum confirming the presence of La, Th, Fe, As and O.

3. Results and discussion

Figure 1(i) shows the powder x-ray diffraction patterns of the sample with nominal compositions $La_{1-x}Th_xFeAsO$ ($x = 0.1$ and 0.2), $La_{1-\delta}FeAsO$ ($\delta = 0.1$ and 0.2) and $LaFeAsO_{1-\delta}$ ($\delta = 0.1$ and 0.2). The La-and O-deficient compounds ($La_{1-\delta}FeAsO$ and $LaFeAsO_{1-\delta}$) crystallize in the tetragonal ZrCuSiAs-type structure and all the reflections could be indexed satisfactorily. The refined lattice parameters for the $La_{1-\delta}OFeAs$ ($\mathbf{a} = 4.0279(8)$ Å, $\mathbf{c} = 8.731(4)$ Å for $\delta = 0.1$ and $\mathbf{a} = 4.0265(9)$ Å, $\mathbf{c} = 8.728(3)$ Å for $\delta = 0.2$) and $LaO_{1-\delta}FeAs$ ($\mathbf{a} = 4.0286(9)$ Å, $\mathbf{c} = 8.734(5)$ Å for $\delta = 0.1$ and $\mathbf{a} = 4.0243(8)$ Å, $\mathbf{c} = 8.722(3)$ Å for $\delta = 0.2$) were found to be smaller than the parent LaFeAsO [19] ($a = 4.038$ Å, $c = 8.753$ Å), which is to be expected since the lanthanum and oxygen deficiency leads to a decrease in the lattice parameters.

The Th-doped compositions ($La_{1-x}Th_xFeAsO$ ($x = 0.1$ and 0.2)) could also be indexed in the tetragonal cell. The refined lattice parameters ($\mathbf{a} = 4.022(1)$ Å and $\mathbf{c} = 8.729(4)$ Å for $x = 0.1$ and $\mathbf{a} = 4.018(1)$ Å and $\mathbf{c} = 8.713(6)$ Å for $x = 0.2$) for Th-doped LaFeAsO were smaller than those reported for pure LaFeAsO, which is due to the incorporation of the smaller thorium ions at the lanthanum sites. A minor amount of ThO_2 can be seen in the powder XRD pattern (figure 1(i)). This suggests that the compositions would be slightly deficient in Th compared to the loaded composition. It should be noted that the earlier reports of Th-doped GdFeAsO, TbFeAsO and NdFeAsO superconductors also report the presence of ThO_2 as

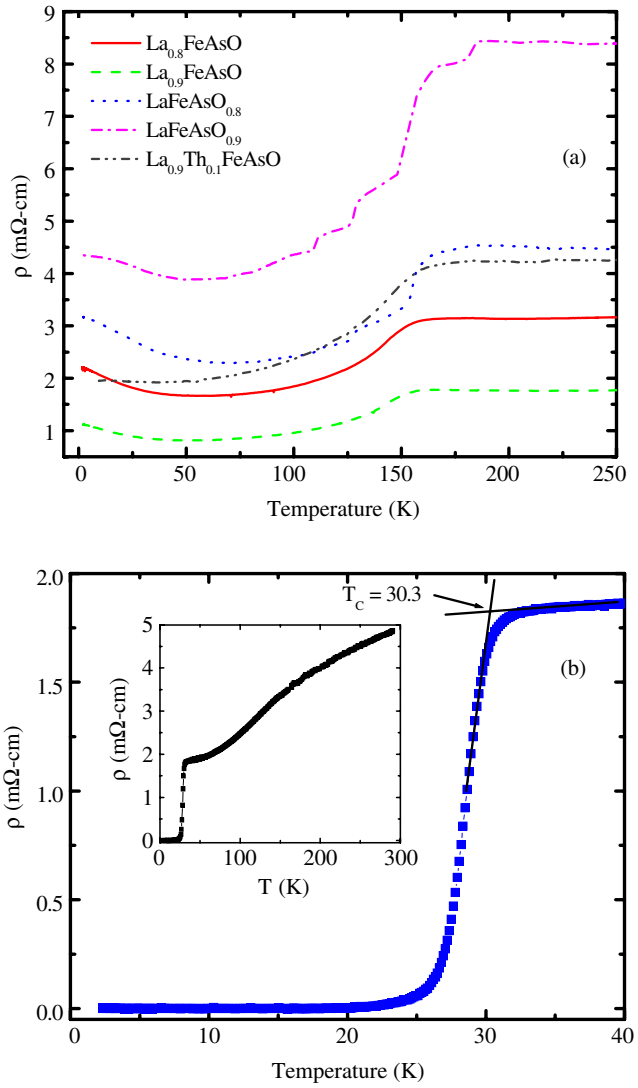

Figure 2. (a) The temperature dependence of resistivity (ρ) as a function of temperature for (a) $La_{0.8}FeAsO$, (b) $La_{0.9}FeAsO$, (c) $LaFeAsO_{0.8}$, (d) $LaFeAsO_{0.9}$ and (e) $La_{0.9}Th_{0.1}FeAsO$. (b) The variation of zero-field resistivity (ρ) with respect to temperature in $La_{0.8}Th_{0.2}FeAsO$. The inset shows resistivity up to room temperature.

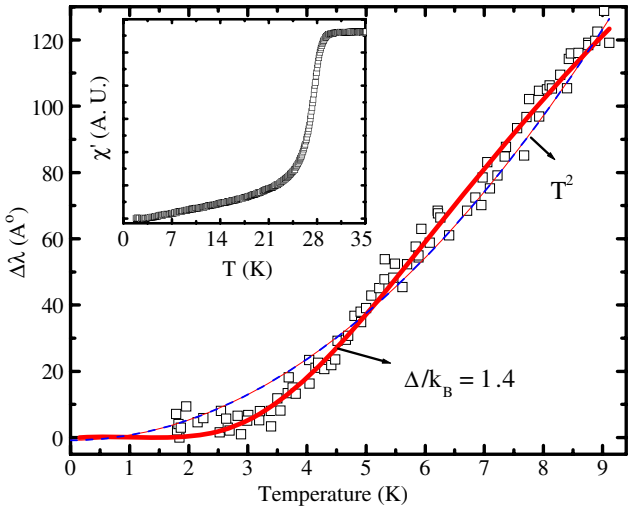

Figure 3. Low temperature (<9 K) variation of penetration depth $\Delta\lambda(T)$ in polycrystalline $La_{0.8}Th_{0.2}FeAsO$. The red line and blue line show the exponential and power law (T^2) fitting, respectively. The inset shows the temperature dependence of the inductive part of rf susceptibility up to 35 K attesting to the onset of bulk diamagnetism at T_c.

a secondary phase [14–16]. It is to be noted that the **a** lattice parameter in $La_{0.8}Th_{0.2}FeAsO$ is lower than that reported for the oxygen-deficient $LaFeAsO_{0.85}$ (**a** = 4.022(2) Å and **c** = 8.707(1) Å) superconductor (T_c = 31.2 K) obtained under high pressure [20] which results in an increase of chemical pressure on the Fe–As plane. The study of Ren *et al* indicated that non-fluorine oxypnictide superconductors could be obtained by using high pressure (6 GPa) synthesis and a further increase in chemical pressure by substituting smaller ions in the Ln–O layers (in turn affecting the Fe–As layers) leads to enhancement of T_c [20]. In figure 1(ii), we show the energy-dispersive x-ray (EDX) spectrum of $La_{0.8}Th_{0.2}FeAsO$, which confirms the presence of La, Th, Fe, As and O in the desired atomic ratio.

The zero-field resistivity as a function of temperature is shown in figure 2 as measured by the standard four-probe method. Figure 2(a) shows the temperature dependence of resistivity for the lanthanum- and oxygen-deficient LaFeAsO compounds along with the resistivity of $La_{0.9}Th_{0.1}FeAsO$. All the samples exhibit a sudden decrease of resistivity at ∼150 K. The resistivity continues to decrease below 150 K and shows a minimum at ∼70 K. However, for $La_{0.9}Th_{0.1}FeAsO$ the resistivity becomes almost independent of temperature (below ∼50 K). Ren *et al* [20] have earlier reported the synthesis of non-superconducting $LaFeAsO_{0.85}$ at ambient pressure which is similar to the behavior of the oxygen-deficient oxypnictides $LaFeAsO_{1-\delta}$ ($\delta = 0.1$ and 0.2) prepared by us. These results confirm that the oxygen and lanthanum deficiency does not induce superconductivity in these La-based oxypnictides prepared at ambient pressure. Figure 2(b) shows the zero resistivity measurement with respect to temperature for $La_{0.8}Th_{0.2}FeAsO$. The inset of this figure shows the variation of resistivity up to room temperature. The resistivity decreases monotonically with decreasing temperature and a rapid drop was observed at 30.3 K showing the onset of superconductivity. The offset ($T_c(0)$) was found to be 26.7 K. The criteria used for determination of transition temperature has been reported earlier [17] and schematically shown in figure 2(b). To confirm the presence of diamagnetic behavior, we measured the inductive part of susceptibility up to 35 K on the same sample. The inset of figure 3 shows the temperature dependence of the inductive part of the magnetic susceptibility using the rf penetration depth technique. This attests to the appearance of superconductivity in this polycrystalline sample. The broadening of the magnetic transition indicates a certain degree of inhomogeneity in the polycrystalline sample, which also explains the observation of slightly lower magnetization onset T_c (by ∼1.8 K) as compared to the resistivity T_c. The inhomogeneity (primarily due to grain boundaries) of the sample is also clear from

the value of the residual resistivity value (RRR $= \rho_{300}/\rho_{31}$) of 2.76. Nevertheless, we emphasize that the onset of superconductivity in $La_{0.8}Th_{0.2}FeAsO$ represents the highest transition temperature in La-based oxypnictides synthesized at ambient pressure.

To get more insight into the pairing mechanism in this multiband superconductor, we plot the shift in rf penetration depth frequency as a function of temperature (figure 3). This dependence is directly related to the anisotropy of the superconducting energy gaps. It has to be pointed out that the technique of rf penetration depth works better for sintered polycrystalline samples as compared to point contact or tunneling techniques [21], as the length scale probed here are two orders of magnitude higher for high κ materials such as the oxypnictides. Further, complications arising out of phonon and magnetic impurities that dominate specific heat and thermal conductivity data are absent here [22].

The BCS expression for the temperature dependence of penetration depth for an isotropic s-wave pairing is given by

$$\Delta\lambda(T) = \lambda(0)\sqrt{\frac{\pi\Delta(0)}{2T}}\exp[-\Delta(0)/T] \qquad (1)$$

where $\Delta\lambda(T)$ is the difference between penetration depth at temperature T and at the lowest measurement temperature of 1.8 K. $\lambda(0)$ and $\Delta(0)$ are the zero temperature values of penetration depth and energy gap, respectively. In the tunnel diode oscillator technique, the change in penetration depth is related to the measured shift in frequency, $\Delta\lambda = -G\Delta f$, where G is a geometrical constant that is calibrated to be $\sim$10 for our set-up. This was estimated by deriving the skin depth ($\delta = 1/\mu_0\pi\sigma f$, σ being the conductivity) from the frequency shift for oxygen-free high purity copper in a shape roughly similar to the superconducting specimen. Because of the uncertainty in geometry, the absolute value of penetration depth is only an approximation but the temperature dependence of the change in penetration depth does not suffer from such problems. The symmetry of the order parameter is an important parameter for understanding the mechanism involved for superconductivity and several experiments using this technique have been reported to address these questions in this new class of superconductors. Hunte *et al* [23] have shown that $LaFeAsO_{0.9}F_{0.1}$ exhibits signs of two-gap behavior similar to that in MgB_2. Shan *et al* [21] have reported the result of point contact spectroscopy (PCAS) which is best described for a p-wave or d-wave gap with a maximum gap of 3.9 $\pm$ 0.7 meV. Gang *et al* [24] reported specific heat measurements for $LaFeAsO_{0.9}F_{0.1-\delta}$ which showed the maximum gap 3.4 $\pm$ 0.5 meV based on the d-wave mode. The penetration depth results of Malone *et al* showed a fully gapped Fermi surface with two gaps that closed at T_c, similar to MgB_2. On the other hand, NdFeAs(O/F) single crystals were reported to have a single anisotropic gap with exponential temperature dependence [25]. In the very recent past, there have been several reports using Andreev reflection, angle-resolved photoemission spectroscopy and scanning tunneling spectroscopic techniques to study the symmetry of the gap and to find if there is more than one gap in this mutiband system. Using point contact Andreev reflection,

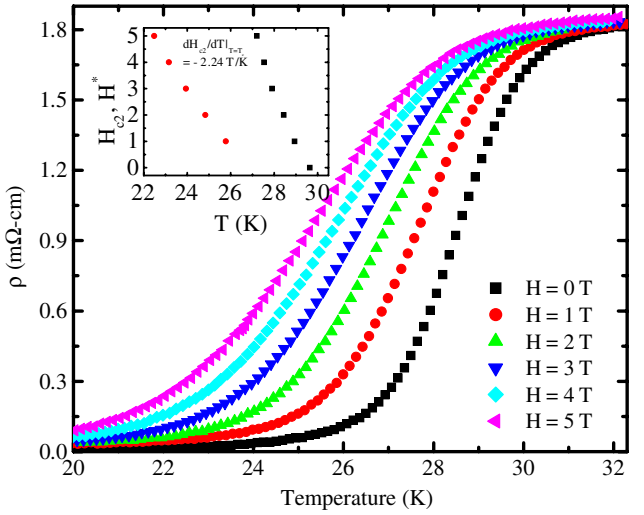

Figure 4. Temperature dependence of the electrical resistivity of $La_{0.8}Th_{0.2}FeAsO$ superconductors under varying magnetic fields. Insets show temperature dependence of upper critical field (■) and irreversibility field (●) as a function of temperature.

Gonnelli *et al* [26] have reported complex and unconventional superconductivity in $LaFeAsO_{1-x}F_x$ with two more energy scales along with a nodeless gap that closed at T_c. In the case of $NdFeAsO_{0.9}F_{0.1}$, a detailed angle-resolved photoelectron spectroscopic study suggests a single gap with very weak anisotropic characteristics [27]. A recent review by Karpinski *et al* suggests a two-gap scenario on the basis of Andreev reflection and STM measurements on $SmFeAsO_{0.8}F_{0.2}$ single crystals [28]. While most of the studies have ruled out the possibility of a cuprate-like d-wave pairing mechanism, the evidence for a multi-gap feature is controversial. In figure 3 we show our rf penetration depth data in the range $0 < T/T_c < 0.3$ for the $La_{0.8}Th_{0.2}FeAsO$ superconductor. We fit the data for an isotropic s-wave gap and a d-wave power law (T^2) dependence. The solid line in figure 3 shows a fitting curve for an isotropic single-gap model that evidently yields better fitting ($R^2 = 0.99$) to the experimental data according to equation (1) with the gap value of $\Delta_0/k_B = 16.6$ (gap $\sim$1.4 meV). We note that, while fitting the data to equation (1) will yield the true estimate of the low lying gap, more information on the possibility of multiple gaps and anisotropy will need analysis of the superfluid density ($\lambda^2(0)/\lambda^2(T)$). Since the sample has a transition temperature at 30.3 K, we calculate $\Delta_0/k_BT_c = 0.54$ and note that this value is smaller than the weak-coupling s-wave BCS value of 1.76. This is suggestive of a gap anisotropy or multiple gaps as in MgB_2 [29] ($\Delta_0/k_BT_c = 0.76$). The multi-gap behavior in LaFeAs(O/F) has also been substantiated from the very high upper critical field indicated in high field transport measurements [23]. A universal two-gap feature for La-based oxypnictide is also indicated from nuclear quadrupole measurements on $LaFeAsO_{0.92}F_{0.08}$, as reported by Kawasaki *et al* [30]. In the inset we show the temperature variation of rf penetration depth for the entire superconducting temperature range.

To obtain the upper critical field (H_{c2}) we have studied the temperature dependence of the resistivity under different

magnetic fields (figure 4). With increasing field, the transition temperature (T_c) shifts to lower values and the transition width gradually becomes broader, similar to the high T_c cuprate superconductors [31]. This suggests the strong anisotropy of the critical field and possible propensity to thermally activated vortex dynamics [32]. The width of the in-field superconducting transition indicates a broad region of flux-flow resistivity. Using the criteria of 90% and 10% of normal state resistivity (ρ_n), we obtained the upper critical field H_{c2} and the irreversibility field $H^*(T)$ (field corresponding to the suppression of bulk critical current density). The H–T phase diagram for sample ($La_{0.8}Th_{0.2}FeAsO$) is shown in the inset of figure 4. We note that these are approximate estimations. Further, by using the Werthamer–Helfand–Hohenberg (WHH) formula $H_{c2}(0) = -0.693T_c\ (dH_{c2}/dT)_{T=T_c}$ [33], the zero-field upper critical field $H_{c2}(0)$ can be calculated. A slope of -2.23 for dH_{c2}/dT was estimated from the H–T phase diagram. Using $T_c = 30.3$ K, we obtain $H_{c2} = 47$ T. It is to be noted that the WHH formula is strictly valid only for a single-band scenario and its use in the present case yields only an approximate extrapolation closer to the lower bound [32]. From the extrapolated value of $H_{c2}(0)$, we can calculate the mean-field Ginzberg–Landau coherence length $\xi = (\Phi_0/2\pi H_{c2}(0))^{1/2}$. Using $\Phi_0 = 2.07 \times 10^{-7}$ G cm^2 and the $H_{c2}(0)$ value, we obtain a coherence length ~26 Å. This value is higher than that reported for LaFeAs(O/F) [12] using single-band approximations.

Since bulk superconductivity was realized by thorium doping in place of La, it is expected to be an electron-doped superconductor. However, in a multiband scenario, both electron and hole pockets are possible. In order to confirm the dominant conduction mechanism, we have carried out studies on the temperature dependence of thermoelectric power (S) (figure 5). The thermoelectric power drops sharply to zero below the superconducting transition temperature. Also the negative value of the thermoelectric power indicates that its major carriers are electron-like (n type), similar to that in LaFeAs(O/F) superconductor [17] and is in contrast to the hole-like carriers observed in (K/Sr)Fe_2As_2 [34]. At room temperature, the value of the thermopower is $-16\ \mu V\ K^{-1}$ and shows a minimum at 90 K ($S = -73.1\ \mu V\ K^{-1}$). It is very interesting to note that the profile of the S versus T curve is similar to that of the low charge density metals like underdoped high T_c cuprates except for the negative sign. We also note that the minima of the negative thermopower shift to lower temperature with Th doping as compared to F-doped LaFeAsO [17]. Further, the inset of figure 5 shows zero-field resistivity above T_c that exhibits a quadratic temperature dependence $\rho = \rho_0 + BT^2$ in the temperature range of T between 31 and 150 K. Here ρ_0 is the residual resistivity determined from the impurity scattering process. The T^2 dependence of ρ below 150 K is reminiscent of the dominant electron–electron scattering process. From the experimental data, the values of $\rho_0 = 1.72$ mΩ cm and $B = 7.49 \times 10^{-5}$ mΩ cm K^{-2} were estimated. We note that the value of the slope B extracted here is larger than the reported value for LaFeAs(O/F) [17] and both $\rho(T)$ and $S(T)$ suggest a stronger dominance of electron correlation effects in the Th-doped superconductor.

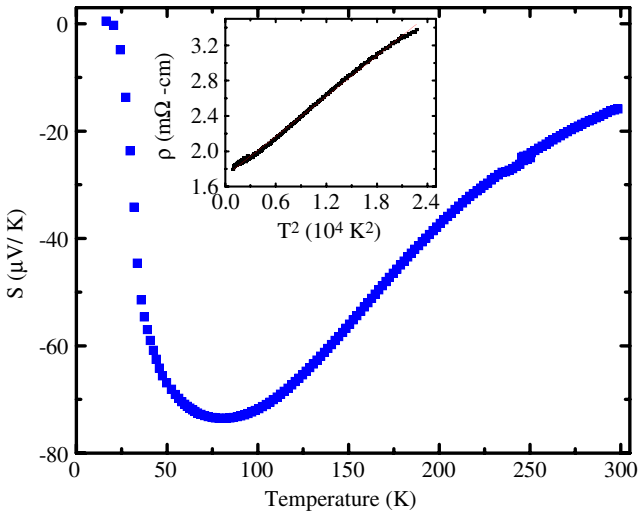

Figure 5. Temperature-dependent thermoelectric power for the sample $La_{0.8}Th_{0.2}FeAsO$. The inset shows the in-plane electrical resistivity of $La_{0.8}Th_{0.2}FeAsO$ as a function of temperature under zero field and the fit of data for 31 K $\leqslant T \leqslant$ 150 K to the form $\rho = \rho_0 + BT^2$.

In summary, we have synthesized three series of oxypnictide compounds with nominal compositions of $La_{1-x}Th_xFeAsO$ ($x = 0.1$ and 0.2), $La_{1-\delta}FeAsO$ ($\delta = 0.1$ and 0.2) and $LaFeAsO_{1-\delta}$ ($\delta = 0.1$ and 0.2) by the high temperature sealed tube method. Lanthanum- and oxygen-deficient compounds were found to be semimetallic like the parent LaFeAsO oxypnictides. A new superconducting oxypnictide ($La_{0.8}Th_{0.2}FeAsO$) was obtained by substituting the trivalent La ion with the tetravalent Th ions in LaFeAsO. This shows the highest transition temperature of 30.3 K in the lanthanum-based oxypnictides synthesized at ambient pressure by electron doping. The temperature dependence of the penetration depth shows exponential behavior and the best fit is obtained for an s-wave pairing mechanism with a gap value of 1.4 meV. Thermoelectric power measurement indicates that the dominant carriers are like electrons. Both thermopower and resistivity studies indicate the presence of strong electron–electron correlation as compared to the F-doped or O-deficient LaFeAsO. From magnetoresistance studies we found $H_{c2}(0)$ values of over 47 T that correspond to a coherence length of 26 Å for this new superconductor.

Acknowledgments

AKG and SP thank DST, Government of India for financial support. JP and SJS thank CSIR and UGC, Government of India, respectively, for fellowships. We thank AIF, JNU for the EDAX measurements.

References

[1] Kamihara Y, Watanabe T, Hirano M and Hosono H 2008 *J. Am. Chem. Soc.* **130** 3296–7
[2] Ma F and Lu Z-Y 2008 *Phys. Rev.* B **78** 033111
[3] Dong J *et al* 2008 *Europhys. Lett.* **83** 27006

[4] Cruz C *et al* 2008 *Nature* **453** 899–902
[5] McGuire A M, Christianson A D, Sefat A S, Jin R, Payzant E A, Sales B C, Lumsden M D and Mandrus D 2008 *Phys. Rev.* B **78** 094517
[6] Chen G F, Li Z, Wu D, Li G, Hu W Z, Dong J, Zheng P, Luo J L and Wang N L 2008 *Phys. Rev. Lett.* **100** 247002
Prakash J, Singh S J, Patnaik S and Ganguli A K 2008 *Physica* C **469** 82–5
[7] Chen X H, Wu T, Wu G, Liu R H, Chen H and Fang D F 2008 *Nature* **453** 761–2
[8] Ren Z-A *et al* 2008 *Europhys. Lett.* **82** 57002
[9] Ren Z-A, Yang J, Lu W, Yi W, Che G-C, Dong X-L, Sun L-L and Zhao Z-X 2008 *Mater. Res. Innov.* **12** 105–6
[10] Yang J *et al* 2008 *Supercond. Sci. Technol.* **21** 082001–3
[11] Takahashi H, Igawa K, Arii K, Kamihara Y, Hirano M and Hosono H 2008 *Nature* **453** 376–8
[12] Prakash J, Singh S, Samal S, Patnaik S and Ganguli A K 2008 *Europhys. Lett.* **84** 57003
[13] Prakash J, Singh S J, Patnaik S and Ganguli A K 2008 *Solid State Commun.* **149** 181–3
[14] Wang C *et al* 2008 *Europhys. Lett.* **83** 67006
[15] Li L, Li Y, Ren Z, Luo Y, Lin X, He M, Tao Q, Zhu Z, Cao G and Xu Z 2008 *Phys. Rev.* B **78** 132506
[16] Xu M, Chen F, He C, Ou H-W, Zhao J F and Feng D L 2008 *Chem. Mater.* **20** 7201–4
[17] Sefat A S, Mcquire M A, Sales B C, Jin R, Howe J Y and Mandrus D 2008 *Phys. Rev.* B **77** 174503
[18] Patnaik S, Singh K J and Budhani R C 1999 *Rev. Sci. Instrum.* **70** 1494
[19] Quebe P, Terbuchte L J and Jeitschko W 2000 *J. Alloys Compounds* **302** 70–4
[20] Ren Z A *et al* 2008 *Europhys. Lett.* **83** 17002
[21] Shan L, Wang Y, Zhu X, Mu G, Fang L and Wen H-H 2008 *Europhys. Lett.* **83** 57004
[22] Carrington A and Manzano F 2003 *Physica* C **385** 205–14
[23] Hunte F, Jaroszynski J, Gurevich A, Larbalestier D C, Jin R, Sefat A S, MacGuire M A, Sales B C, Christen D K and Mandrus D 2008 *Nature* **453** 903–5
[24] Gang M, Yu Z X, Lei F, Lei S, Cong R and Hu W H 2008 *Chin. Phys. Lett.* **25** 2221–4
[25] Martin C *et al* 2008 arXiv:0807.0876 [cond-mat]
[26] Gonnelli R S, Daghero D, Tortello M, Ummarino G A, Stepanov V A, Kim J S and Kremer R K 2008 arXiv:0807.3149 [cond-mat]
[27] Kondo T *et al* 2008 *Phys. Rev. Lett.* **101** 147003
[28] Karpinski J *et al* 2009 arXiv:0902.0224 [cond-mat]
[29] Manzano F, Carrington A, Hussey N E, Lee S, Yamamoto A and Tajima S 2002 *Phys. Rev. Lett.* **88** 047002
[30] Kawasaki S, Shimada K, Chen G F, Luo J L, Wang N L and Zheng G 2008 *Phys. Rev.* B **78** 220506(R)
[31] Palstra T T M, Batlogg B, Schneemeyer L F and Waszczak J V 1988 *Phys. Rev. Lett.* **61** 1662–5
[32] Patnaik S, Gurevich A, Kaushik S D, Bu S D, Choi J, Eom C B and Larbalestier D C 2004 *Phys. Rev.* B **70** 064503
Gurevich A 2003 *Phys. Rev.* B **67** 184515
[33] Werthamer N R, Helfand E and Hohenberg P C 1966 *Phys. Rev.* **147** 295–302
[34] Sasmal K, Lv B, Lorenz B, Guloy A M, Chen F, Xue Y Y and Chu C W 2008 *Phys. Rev. Lett.* **101** 107007